Optimised Passive Discrete-time Models of Frequency-dependent Loss in Strings

26th International Congress on Sound and Vibration
7-11 July 2019, Montreal

OPTIMISED PASSIVE DISCRETE-TIME MODELS OF FREQUENCY-DEPENDENT LOSS IN LINEAR STRINGS

Charlotte Desvages
Acoustics and Audio Group
School of Mathematics, University of Edinburgh, UK
email: charlotte.desvages@ed.ac.uk

Stefan Bilbao
Acoustics and Audio Group
Reid School of Music, University of Edinburgh, UK

String vibration forms the basis for a wide variety of physical modelling sound synthesis environments. Direct simulation in the space-time domain (through techniques such as, for example, the finite difference time domain method) allows for great generality and flexibility, particularly if one is concerned with essential nonlinear features such as, e.g., nonlinear excitation or collisions. Both theoretical and experimental investigations have shown that decay times of linear string transverse modes are frequency-dependent in a nontrivial way. This profile plays an important role in the perceived realism of the synthetic sound, but is nontrivial to reproduce in a pure space-time domain framework. Recent work has demonstrated different approaches to tackle similar problems, sharing a common principle: the impedance of the lossy part of the system is approximated by the input impedance of a network of passive circuit elements, with a readily available time-domain realisation. This paper outlines a procedure for optimising the parameters of such a model against a reference loss profile, which may come from a theoretical model or from experimental measurements of string decay times. Passivity is ensured by enforcing positive-realness of the approximated impedance. The corresponding time domain system is then translated to the discrete time setting; a finite difference scheme is chosen such that the passivity property is preserved, leading to guarantees of numerical stability. The decay times of the transverse modes of simulated plucked strings are measured and compared to the original data, in order to assess the fidelity of the reproduced loss profile, at different orders of approximation.
Keywords: strings, impedance, decay, finite difference, simulation

1. Introduction

Physical modelling has established itself as a popular method for high-quality sound synthesis. In particular, time-stepping methods based upon discretisation of the continuous space-time partial differential equations characterising the system (e.g., using the finite difference method [1, 2]) allow for great generality and flexibility when modelling complex, potentially nonlinear phenomena. Tackling string sound synthesis under this framework first requires accurate modelling of its linear behaviour, before addressing these more complex issues. When transverse string vibration is concerned, an important aspect of this behaviour is the frequency-dependent attenuation of the transverse modes — careful reproduction of this loss profile is crucial when targeting high-quality sound synthesis. However, this is not a trivial task in such a time-domain framework.

Many attempts at modelling arbitrary frequency-dependent dynamic behaviour have been made in the space-time domain. Of particular interest to musical acoustics are studies on viscothermal losses in acoustic pipes [3, 4, 5], frequency-dependent absorbing boundary conditions in room acoustics simulations [6], and time-domain simulation of viscoelastic dynamic behaviour through optimised one-pole digital filters [7] — this last approach is indeed similar to that presented in this work. When the more specific problem of stiff string damping is concerned, the two-parameter models by Ruiz and Hiller [8], used in e.g. [9], and by Bensa *et al.* [10], seen in e.g. [11, 12], have been popular approaches, but remain unsatisfactory if one is concerned with accurate reproduction of the frequency dependence of decay rates across the spectrum. This paper presents a method to accurately reproduce the frequency-dependent loss profile characterising linear transverse string vibration, in purely time-domain simulation results. A passive discrete-time domain system is designed to emulate damping processes with the impedance of a lumped element circuit model. The parameters of this model are optimised so as to most accurately approximate the target loss profile, while keeping the order of approximation as low as possible. Section 2 describes the general model (and related assumptions) of damped linear string vibration. Section 3 describes the approximated impedance in terms of lumped element circuit modelling. Section 4 outlines the finite difference scheme employed for time-domain simulations, with an emphasis on stability properties. Finally, Sections 5 and 6 present optimisation and simulation results to validate the approach taken.

2. Continuous-time linear stiff string model

2.1 Lossless system

Consider the transverse displacement $w(x,t)$ of a stiff string (expressed in m), assumed to vibrate in a single polarisation, defined along spatial coordinate $x \in \mathbb{R}$ and time $t \in \mathbb{R}_{\geqslant 0}$. In the lossless case, $w(x,t)$ solves a linear partial differential equation (PDE)

$$\mathcal{L}w = 0, \tag{1}$$

where $\mathcal{L}$ is a partial differential operator. For instance, the Euler-Bernoulli model defines $\mathcal{L}$ as

$$\mathcal{L} := \rho_L \partial_t^2 - T\partial_x^2 + EI_0\partial_x^4, \tag{2}$$

where ρ_L is the linear mass density (kg/m), T the tension (N), E Young's modulus (Pa), I_0 the area moment of inertia (m^4), and $\partial_t^m, \partial_x^m$ designate the m^{th} order partial differential operators with respect to time and space, respectively. The frequency-domain characteristic equation, assuming a test solution $w(x,t) := e^{st+j\beta x}$ in terms of complex frequency $s = \sigma + j\omega \in \mathbb{C}$ and wavenumber $\beta \in \mathbb{R}$, is given by

$$\hat{\mathcal{L}} = 0, \qquad \hat{\mathcal{L}} := \rho_L s^2 + T\beta^2 + EI_0\beta^4, \tag{3}$$

where $\hat{\mathcal{L}}$, a polynomial in s and $j\beta$, is the frequency-domain counterpart of $\mathcal{L}$.

2.2 Damped system: general model

Now, let $Z(s) \in \mathbb{C}$ be an impedance per unit length, characterising damping processes in the stiff string. The corresponding force per unit length is linearly related to the string velocity. Incorporating this force term into the string model therefore leads to a general characteristic equation given by

$$\hat{\mathcal{L}} + sZ(s) = 0. \tag{4}$$

The approach to loss modelling outlined in this paper stems from passive network synthesis theory [13]. The impedance $Z(s)$ characterising damping mechanisms in linear stiff string vibration is approximated

by the finite-order rational driving-point impedance $Z_{\boldsymbol{\chi}}(s)$ of a one-port passive lumped element circuit model. Substituting $Z(s) \approx Z_{\boldsymbol{\chi}}(s)$ in Eq. (4) yields

$$\hat{\mathcal{L}} + sZ_{\boldsymbol{\chi}}(s) \approx 0. \tag{5}$$

This impedance is parametrised by $\boldsymbol{\chi} \in \mathbb{R}^{N_\chi}$ (with $N_\chi \leqslant N_\omega$), the elements of which correspond to the values of the passive electrical elements in the circuit. The goal is then to find optimal such values, so that $Z_{\boldsymbol{\chi}}(s)$ closely approximates $Z(s)$, while keeping N_χ small.

The model proposed for damped string motion must be passive, i.e. dissipate energy — all solutions for the transverse displacement of the string must decay over time, in the absence of forcing terms. This means that all solutions of Eq. (5) must verify $\mathrm{Re}\,(s) = \sigma \leqslant 0$.

2.3 Positive-real functions

Cauer [14] established that a one-port circuit is guaranteed passive if its driving-point impedance $Z(s)$ is *positive-real* (PR), that is

$$\begin{cases} \mathrm{Re}\,(s) > 0 & \Rightarrow \quad \mathrm{Re}\,(Z(s)) \geqslant 0, \quad \text{and} \\ \mathrm{Im}\,(s) = 0 & \Rightarrow \quad \mathrm{Im}\,(Z(s)) = 0. \end{cases} \tag{6}$$

Brune [15] restricted the definition of PR functions to rational functions of s, for which both the numerator and denominator polynomials verify the conditions given in Eq. (6). This further restriction guarantees that the input impedance is realisable as that of a one-port network of a finite number of circuit elements. For the rest of this paper, mentions of PR functions will refer to this rational definition.

2.4 Application to lightly damped string vibration

In the context of musical string vibration, oscillations are lightly damped, and two simplifying assumptions are proposed:

a) Z characterises damping, and is therefore predominantly resistive;
b) losses are small, i.e. $|\sigma| \ll \omega$, and $Z(s) \approx Z(j\omega)$.

The imaginary part of Eq. (4) can therefore be written as

$$\begin{aligned} & 2\rho_L\sigma\omega + \mathrm{Im}\,(sZ(j\omega)) \approx 0 \\ \Rightarrow \quad & 2\rho_L\sigma\omega + \omega\mathrm{Re}\,(Z(j\omega)) + \underbrace{\sigma\mathrm{Im}\,(Z(j\omega))}_{\text{small, by a) and b)}} \approx 2\rho_L\sigma\omega + \omega\mathrm{Re}\,(Z(j\omega)) \approx 0 \end{aligned} \tag{7}$$

It is therefore possible to relate the frequency-dependent mechanical resistance $\mathrm{Re}\,(Z(j\omega))$ associated with damping processes to the decay rate σ of the solutions, as

$$\mathrm{Re}\,(Z(j\omega)) \approx -2\rho_L\sigma. \tag{8}$$

For this study, the frequency-dependent decay rate $\sigma(\omega)$ is assumed to be known for a number of frequencies $\omega_i, i = 1, \ldots, N_\omega$, either from an analytical model (e.g. [16]) or from experimental measurements of modal decay times. An optimisation procedure is then employed to fit $\mathrm{Re}\,(Z_{\boldsymbol{\chi}}(j\omega))$ to this data.

In line with b), it is further expected that losses are small enough to not affect the dispersion relation — thus, any dependency of Z on the wavenumber β may be expressed directly in terms of ω, using the lossless dispersion relation $\beta(\omega)$. From Eq. (3), the dispersion relation for the Euler-Bernoulli model is

$$\beta(\omega) \approx \beta_{\mathrm{EB}}(\omega) = \sqrt{\frac{\sqrt{T^2 + 4EI_0\rho_L^2\omega^2} - T}{2EI_0}}. \tag{9}$$

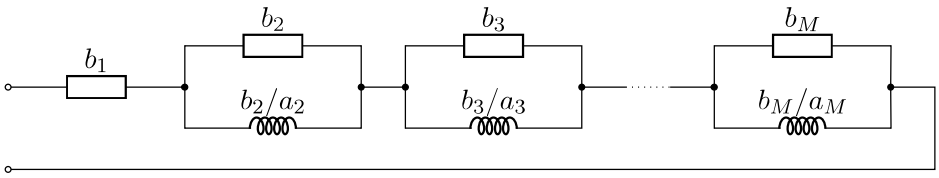

Figure 1: One-port Foster RL network of the second type, corresponding to the driving point impedance $\Gamma(s)$ given in (11), with $a_1 = 0$. The symbol –▭– represents a resistance, while –ᔓᔓᔓ– is an inductance.

3. Approximation with a Foster RL network

Consider a function $Z_{\boldsymbol{\chi}}(s)$ of the form

$$Z_{\boldsymbol{\chi}}(s) := \Gamma(s) + \beta^2 \Xi(s), \tag{10}$$

where $\Gamma(s)$ and $\Xi(s)$ correspond to the input impedance of a canonical Foster RL network [17] (see Fig. 1), that is

$$\Gamma(s) := \sum_{q=1}^{M} \frac{b_q s}{s + a_q} := \sum_{q=1}^{M} \Gamma_q(s) \ , \qquad \Xi(s) := \sum_{q'=1}^{M'} \frac{b'_{q'} s}{s + a'_{q'}} := \sum_{q'=1}^{M'} \Xi_{q'}(s) \ , \qquad b_q,\, a_q,\, b'_{q'},\, a'_{q'} \geqslant 0. \tag{11}$$

The coefficients a_1, a'_1 can be made zero to introduce a frequency-independent term in $\Gamma(s)$ or $\Xi(s)$. As will be seen in Section 4, the addition of terms proportional to β^2 can be interpreted as emulating viscoelastic damping (see, e.g., [18, pp. 225-226]).

The $N_\chi = 2\,(M + M')$ parameters to optimise are therefore

$$\boldsymbol{\chi} := \left[b_1, \ldots, b_M, a_1, \ldots, a_M, b'_1, \ldots, b'_{M'}, a'_1, \ldots, a'_{M'}\right]^\mathsf{T}. \tag{12}$$

A property of PR functions is that the sum of two PR functions is PR. The condition that all elements of $\boldsymbol{\chi}$ are positive is therefore sufficient to ensure that $Z_{\boldsymbol{\chi}}(s)$ is PR, as a sum of PR terms.

In the space-time domain, the system of PDEs associated with the characteristic equation (5), when $Z_{\boldsymbol{\chi}}(s)$ is defined as in Eq. (10), is given by

$$\mathcal{L}w = -\sum_{q=1}^{M} b_q \partial_t \gamma_q + \sum_{q'=1}^{M'} b'_{q'} \partial_t \partial_x^2 \xi_{q'}, \tag{13a}$$

$$\partial_t \gamma_q = \partial_t w - a_q \gamma_q \ , \qquad q = 1, \ldots, M, \tag{13b}$$

$$\partial_t \xi_{q'} = \partial_t w - a'_{q'} \xi_{q'} \ , \qquad q' = 1, \ldots, M', \tag{13c}$$

where each $\gamma_q(x,t)$ and $\xi_{q'}(x,t)$ is defined over the same domain as $w(x,t)$.

4. Translation to the discrete space-time domain

4.1 Finite difference operators

The domain of definition of $w(x,t)$ is discretised into a spatio-temporal grid, characterised by step sizes k (temporal) and h (spatial), both real and positive.

Let the grid function w_l^n be a discrete approximation of $w(x,t)$ at time step $n \in \mathbb{N}_0$ and grid point $l \in \mathbb{Z}$, such that $w(x,t) \approx w(lh, nk)$. Shift operators are defined by their effect on w_l^n, as

$$e_{t\pm} w_l^n := w_l^{n\pm1} \qquad\qquad e_{x\pm} w_l^n := w_{l\pm1}^n \tag{14}$$

Temporal difference operators are defined in terms of $e_{t\pm}$, as

$$\mu_{t\pm} := \frac{e_{t\pm}+1}{2} = 1 + \mathcal{O}(k), \quad \delta_{t\pm} := \pm\frac{e_{t\pm}-1}{k} = \partial_t + \mathcal{O}(k), \quad \delta_{t\cdot} := \frac{e_{t+}-e_{t-}}{2k} = \partial_t + \mathcal{O}(k^2). \tag{15}$$

Spatial difference operators may also be defined as

$$\delta_{x\pm} := \pm\frac{e_{x\pm}-1}{h} = \partial_x + \mathcal{O}(h), \qquad \delta_{xx} := \delta_{x+}\delta_{x-} = \partial_x^2 + \mathcal{O}(h^2). \tag{16}$$

4.2 Finite difference scheme

Let L be a difference operator approximating the partial differential operator $\mathcal{L}$ defined by Eq. (2). A finite difference scheme for the lossless stiff string problem may thus be defined as

$$\mathsf{L}w_l^n = 0. \tag{17}$$

Now, a finite difference scheme for the damped stiff string problem defined by Eq. (13) is given by

$$\mathsf{L}w_l^n = -\sum_{q=1}^{M} b_q \delta_{t+}\gamma_{q,l}^{n-1/2} + \sum_{q'=1}^{M'} b'_{q'}\delta_{t+}\delta_{xx}\xi_{q',l}^{n-1/2}, \tag{18a}$$

$$\delta_{t+}\gamma_{q,l}^{n-1/2} = \delta_{t\cdot}w_l^n - a_q\mu_{t+}\gamma_{q,l}^{n-1/2}, \qquad q = 1,\ldots,M, \tag{18b}$$

$$\delta_{t+}\xi_{q',l}^{n-1/2} = \delta_{t\cdot}w_l^n - a'_{q'}\mu_{t+}\xi_{q',l}^{n-1/2}, \qquad q' = 1,\ldots,M'. \tag{18c}$$

where $\gamma_{q,l}^{n-1/2}$, $\xi_{q',l}^{n-1/2}$ are grid functions defined over the same grid, but shifted from w_l^n by $1/2$ time step.

4.3 Frequency-domain analysis

Assuming a discrete test solution of the form $w_l^n := z^n e^{j\beta lh}$, where $z := e^{sk}$, the discrete-time characteristic equation for Scheme (18) is

$$\hat{\mathsf{L}} + \frac{z-z^{-1}}{2k}\tilde{Z}_{\boldsymbol{\chi}}(\tilde{s}) = 0, \tag{19}$$

where $\hat{\mathsf{L}}$, the frequency-domain counterpart of L, is a polynomial in z and $e^{j\beta h}$. The discrete-time impedance $\tilde{Z}_{\boldsymbol{\chi}}(\tilde{s})$ is given by

$$\tilde{Z}_{\boldsymbol{\chi}}(\tilde{s}) := \Gamma(\tilde{s}) + \tilde{\beta}^2\Xi(\tilde{s}), \tag{20}$$

where the functions Γ, Ξ are defined as in Eq. (11), and $\tilde{s}$, $\tilde{\beta}$ are defined as

$$\tilde{s} := \frac{2}{k}\frac{z^{1/2}-z^{-1/2}}{z^{1/2}+z^{-1/2}} = \frac{2}{k}\frac{z-1}{z+1}, \qquad \tilde{\beta} := \frac{2}{h}\sin\left(\frac{\beta h}{2}\right). \tag{21}$$

Note that the choice of $\tilde{s}$ given in Eq. (21) corresponds to a bilinear transform mapping of the s-plane to the z-plane. In particular, the bilinear transform maps the left half-s-plane to the unit disk in the z-plane, meaning that positive-realness is preserved after temporal discretisation; in other words, if $Z_{\boldsymbol{\chi}}(s)$ is PR, then $Z_{\boldsymbol{\chi}}(\tilde{s})$ is PR. Furthermore, note that $\tilde{\beta}^2 \geqslant 0$, and therefore, by Eq. (20), $\tilde{Z}_{\boldsymbol{\chi}}(\tilde{s})$ is also PR.

Now, assume a choice of difference operator L such that

$$\mathrm{Re}\left(\left(z-z^{-1}\right)^*\hat{\mathsf{L}}\right) > 0 \quad \forall\,|z|>1, \beta\in\mathbb{R}, \tag{22}$$

where * denotes complex conjugation. It follows from Eq. (22) that $\hat{\mathsf{L}}$ has no roots $z = e^{sk}$ outside the unit disk, and therefore that the lossless discrete system (17) is passive[1]. Indeed, assume that there exists a zero $z_0 := e^{\sigma_0 k} e^{j\omega_0 k}$ of $\hat{\mathsf{L}}$ such that $|z_0| > 1$. One therefore has $\mathrm{Re}\left(\left(z_0 - z_0^{-1}\right)^* \hat{\mathsf{L}}(z_0)\right) = \mathrm{Re}\,(0) = 0$, which directly contradicts Eq. (22), and the implication follows.

It can be similarly shown that the lossy discrete system, given in the time-domain by Eqs. (18), has no unbounded solutions, i.e. that all solutions z of Eq. (19) are inside the unit disk. Assume that there exists a solution z_0 to Eq. (19) such that $|z_0| > 1$. Multiplying Eq. (19) by $\left(z_0 - z_0^{-1}\right)^*$ and examining the real part leads to

$$\underbrace{\mathrm{Re}\left(\left(z_0 - z_0^{-1}\right)^* \hat{\mathsf{L}}(z_0)\right)}_{>0,\text{ by assumption}} + \underbrace{\frac{\left|z_0 - z_0^{-1}\right|^2}{2k}}_{>0} \underbrace{\mathrm{Re}\left(\tilde{Z}_{\boldsymbol{\chi}}(\tilde{s}_0)\right)}_{>0,\text{ by PR property}} = 0, \quad \text{where } \tilde{s}_0 := \frac{2}{k}\frac{z_0 - 1}{z_0 + 1}. \tag{23}$$

Since all terms on the LHS are strictly positive, Eq. (23) is a contradiction. Scheme (18) is therefore stable under no further restrictions than those imposed on the lossless scheme (17) to satisfy Eq. (22).

5. Objective function and optimisation

Let $\tilde{\sigma} := \mathrm{Re}\,(\tilde{s})$ and $\tilde{\omega} := \mathrm{Im}\,(\tilde{s}) = \frac{2}{k}\tan\left(\frac{\omega k}{2}\right)$, such that $\tilde{s} = \tilde{\sigma} + j\tilde{\omega}$. The bilinear transform mapping given by Eq. (21) maps the infinite imaginary axis in the s-plane to the unit circle in the z-plane, with $\omega = 0$ mapped to $\tilde{\omega} = 0$, and $\omega = \pm\infty$ mapped to $\tilde{\omega} = \pm\frac{\pi}{k}$. As a result, high frequencies are increasingly warped in the discrete-time system — optimising in the continuous-time domain would fail to take this warping into account, and produce distorted simulation results.

Due to the warping of both frequencies and wavenumbers under discretisation, the discrete-time resistance at observed frequency ω and wavenumber β is $\mathrm{Re}(\tilde{Z}_{\boldsymbol{\chi}}(j\tilde{\omega}))$. The parameters $\boldsymbol{\chi}$ should therefore be optimised so as to minimise the distance between $\mathrm{Re}(Z(j\omega))$ and $\mathrm{Re}(\tilde{Z}(j\tilde{\omega}))$.

The objective function to minimise is given by

$$E(\boldsymbol{\chi}) = \sum_{i=1}^{N_\omega} \left(\frac{\mathrm{Re}(\tilde{Z}_{\boldsymbol{\chi}}(j\tilde{\omega}_i)) - \mathrm{Re}(Z(j\omega_i))}{\mathrm{Re}(Z(j\omega_i))} \right)^2. \tag{24}$$

In the following results, the reference loss profile $\mathrm{Re}(Z(j\omega))$ is given by the physical model described in [16], incorporating effects of air viscosity, viscoelasticity, and thermoelasticity. A range of $N_\omega = 200$ logarithmically spaced frequencies are selected to cover the audible range. The parameters $\boldsymbol{\chi}$ are initialised with random values, and a change of variables $u \to e^u$ guarantees that they remain positive.

Fig. 2 shows optimisation results for a violin A string and a cello D string. In each subfigure, the top graph shows the reference and optimised loss profiles plotted against frequency $f := \frac{\omega}{2\pi}$, with each $\mathrm{Re}(\Gamma(j\tilde{\omega}))$ and $\mathrm{Re}(\tilde{\beta}^2\Xi(j\tilde{\omega}))$ plotted individually to visualise their contributions. The bottom graph displays the relative error ΔZ between the reference profile and its approximation. The values of M and M' were chosen to be the lowest for which ΔZ did not exceed 1% over the frequency range.

Note that evaluating $\tilde{\omega}$ and $\tilde{\beta}$ requires knowledge of the step sizes k and h. The results in Fig. 2 assume a simple choice for L, given by $\mathsf{L} := \rho_L \delta_{tt} - T\delta_{xx} + EI_0\delta_{xxxx}$. The sample rate is fixed at $F_s = 44.1$ kHz, and the time step is thus $k := \frac{1}{F_s}$. The grid spacing h is chosen to satisfy the stability condition of the lossless Scheme (17).

6. Simulation results

For time-domain simulations, the spatial discrete domain is restricted to a bounded interval, and Scheme (18) is complemented with a set of reflecting boundary conditions. The green crosses in Fig. 3

[1]Note that the satisfaction of Eq. (22) may be contingent on a condition relating the step sizes h and k, in which case their value is chosen so as to satisfy this stability condition.

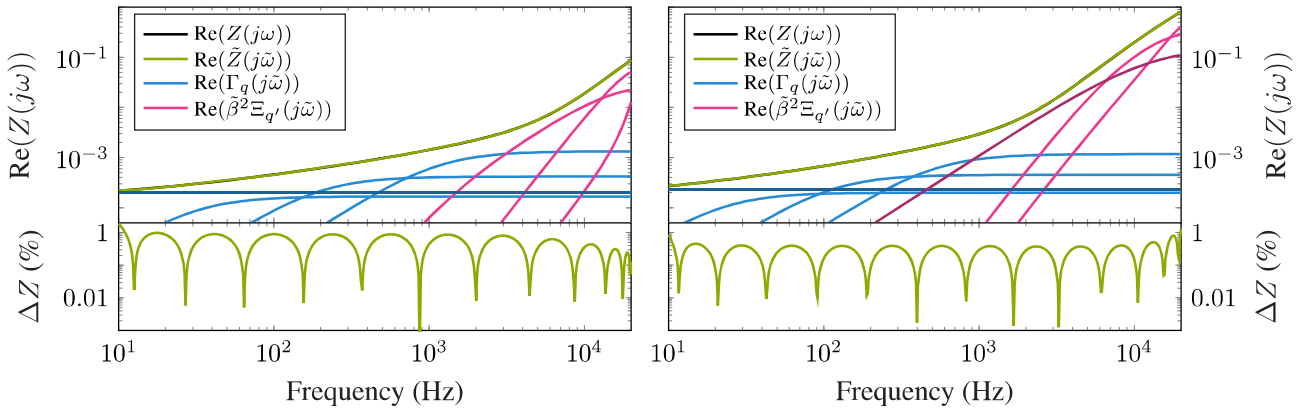

Figure 2: Optimisation results for a violin A string (left) and a cello D string (right): optimised resistance (in green) and reference profile (in black, obscured by the green curve). The Γ_q terms are drawn in blue, the $\Xi_{q'}$ terms in red, with a darker shade indicating terms where $a_q = 0$ or $a'_{q'} = 0$.

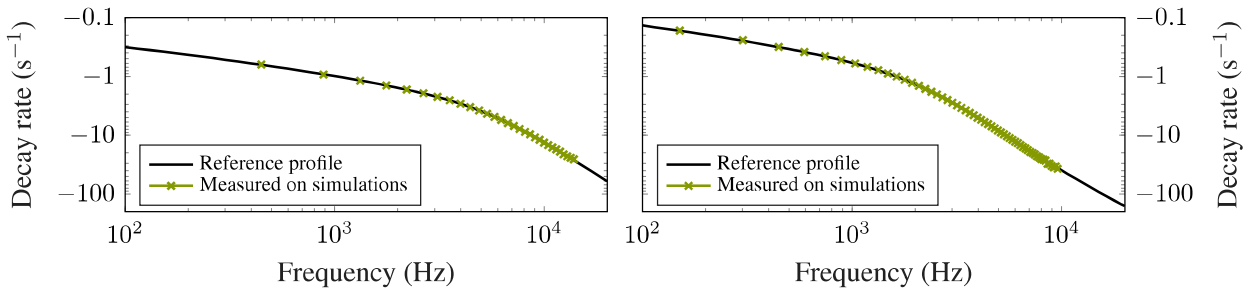

Figure 3: Modal decay rates for a violin A string (left) and a cello D string (right): reference profile (in black) and measured decay rates on time-domain simulations (green crosses), employing Scheme (18) and the optimised parameters $\boldsymbol{\chi}$. Target decay rates are reproduced accurately by the low-order approximation over the whole audible spectrum.

show the modal decay rates measured[2] on simulations of a violin A string and a cello D string, produced using Scheme (18), where L is given by the simple Euler-Bernoulli scheme, and the set of parameters $\boldsymbol{\chi}$ is that extracted from the optimisation procedure described in Section 5. The reference decay rate $\sigma(\omega)$ (black curves in Fig. 3) is given by Eq. (8). As expected from the optimisation results in Section 5, the decay rates measured on simulation results computed using Scheme (18) with optimised parameters are a very good match to the reference profile — in particular, no warping effects are observed. The small losses approximations made in Section 2.4 do not seem to have any significant impact on the accuracy of the results.

7. Conclusion

This paper describes and evaluates a procedure to emulate the frequency-dependent damping of linear transverse string vibration using low-order approximations, constructing a model directly useable in discrete time-domain simulations. The PR property leads to guarantees of passivity — and thus, of

[2]Decay rates were evaluated by linear regression on the modal amplitudes (expressed in dB) as they decreased over time, extracted from spectrograms for 10 simulated waveforms (string displacement read at one point on the string), each arising from randomised initial conditions. This process yielded accurate measurements of decay rates — the 95% confidence intervals would not be visible on the graph.

numerical stability. Modal frequency-dependent decay rates are accurately reproduced in time-domain simulations, at a relatively modestly increased computational cost.

The process described here is readily generalisable in two directions. Firstly, it is independent from the choice of numerical scheme for the lossless system, as long as such scheme satisfies Eq. (22). More elaborate schemes to simulate linear transverse stiff string vibration (such as, e.g., those investigated in [19]) can straightforwardly substitute the difference operator L employed here.

Secondly, it is relatively independent from the reference data against which the model is optimised. Here, in part for brevity, the "ground truth" loss profile was given by an analytical curve, evaluated at many frequency bins. However, such profile may also come from, e.g., experimental measurements of modal decay times. Preliminary results using sparse, noisy data suggest that the procedure is robust to such perturbations — a detailed investigation using experimental data from a wide range of strings would be necessary to confirm this.

REFERENCES

1. Strikwerda, J. C., *Finite difference schemes and partial differential equations*, Siam (2004).
2. Bilbao, S., *Numerical sound synthesis*, John Wiley & Sons, Chichester, UK (2009).
3. Hélie, T. and Matignon, D. Diffusive representations for the analysis and simulation of flared acoustic pipes with visco-thermal losses, *Math. Mod. Meth. Appl. S.*, **16** (4), 503–536, (2006).
4. Thompson, S. C., Gabrielson, T. B. and Warren, D. M. Analog model for thermoviscous propagation in a cylindrical tube, *J. Acoust. Soc. Am.*, **135** (2), 585–590, (2014).
5. Bilbao, S. and Harrison, R. Passive time-domain numerical models of viscothermal wave propagation in acoustic tubes of variable cross section, *J. Acoust. Soc. Am.*, **140** (1), 728–740, (2016).
6. Bilbao, S. and Hamilton, B. Passive volumetric time domain simulation for room acoustics applications, *J. Acoust. Soc. Am.*, **145** (4), 2613–2624, (2019).
7. Parret-Fréaud, A., Cotté, B. and Chaigne, A. Time-domain damping models in structural acoustics using digital filtering, *Mechanical Systems and Signal Processing*, **68**, 587–607, (2016).
8. Ruiz, P. M., *A technique for simulating the vibration of strings with a digital computer*, Ph.D. thesis, University of Illinois at Urbana-Champaign, (1970).
9. Chaigne, A. and Askenfelt, A. Numerical simulations of piano strings. I. A physical model for a struck string using finite difference methods, *J. Acoust. Soc. Am.*, **95** (2), 1112–1118, (1994).
10. Bensa, J., Bilbao, S., Kronland-Martinet, R. and Smith III, J. O. The simulation of piano string vibration: From physical models to finite difference schemes and digital waveguides, *J. Acoust. Soc. Am.*, **114** (2), 1095–1107, (2003).
11. Chabassier, J., Duruflé, M. and Joly, P. Time domain simulation of a piano. Part 2: numerical aspects, *ESAIM: M2AN*, **50** (1), 93–133, (2016).
12. Desvages, C. and Bilbao, S. Two-polarisation physical model of bowed strings with nonlinear contact and friction forces, and application to gesture-based sound synthesis, *Appl. Sci.*, **6** (5), 135, (2016).
13. Kuo, F. F., *Network analysis and synthesis*, John Wiley & Sons, Ltd, 2nd edition edn. (1966).
14. Cauer, W. Die Verwirklichung der Wechselstromwiderstände vorgeschriebener Frequenzabhängigkeit, *Arch. Elektrotechn.*, **17**, 355–388, (1926).
15. Brune, O. Synthesis of a finite two-terminal network whose driving-point impedance is a prescribed function of frequency, *MIT J. Math. Phys.*, **10** (1–4), 191–236, (1931).
16. Valette, C. and Cuesta, C., *Mécanique de la corde vibrante*, Hermès, Paris, France (1993).
17. Foster, R. M. A Reactance Theorem, *Bell Syst. Tech. J.*, **3** (2), 259–267, (1924).
18. Chaigne, A. and Kergomard, J., *Acoustics of musical instruments*, Springer (2016).
19. Ducceschi, M. and Bilbao, S. Conservative finite difference time domain schemes for the prestressed Timoshenko, shear and Euler-Bernoulli beam equations, *Wave Motion*, **89**, 142 – 165, (2019).